Surface and Deep Signal Correlation in a Pediatric Dystonia Case with DBS

Surface and Deep Signal Correlation in a Pediatric Dystonia Case with DBS

Elisa Barbi
Neuroscience and Human Genetics Department, Meyer Children's Hospital IRCCS
Florence, Italy
elisa.barbi@meyer.it

Chiara Rossi
Neuroscience and Human Genetics Department, Meyer Children's Hospital IRCCS
Florence, Italy
chiara.rossi@meyer.it

Edoardo Fino
Neuroscience and Human Genetics Department, Meyer Children's Hospital IRCCS
Florence, Italy.
Neuroscience, Pharmacology and Child Health Department, University of Florence, Italy
edoardo.fino@meyer.it

Simone Peraio
Department of Neurosurgery, Meyer Children's Hospital IRCCS, Florence, Italy
simone.peraio@meyer.it

Andrea Di Rita
Department of Neurosurgery, Meyer Children's Hospital IRCCS, Florence, Italy
andrea.dirita@meyer.it

Alice Noris
Department of Neurosurgery, Meyer Children's Hospital IRCCS, Florence, Italy
alice.noris@meyer.it

Sara Ciabattini
Neuroscience and Human Genetics Department, Meyer Children's Hospital IRCCS
Florence, Italy
sara.ciabattini@meyer.it

Federico Melani
Neuroscience and Human Genetics Department, Meyer Children's Hospital IRCCS
Florence, Italy
federico.melani@meyer.it

Renzo Guerrini
Neuroscience and Human Genetics Department, Meyer Children's Hospital IRCCS, Florence, Italy.
Neuroscience, Pharmacology and Child Health Department, University of Florence, Italy
renzo.guerrini@meyer.it

Flavio Giordano
Epilepsy Surgery and Functional Neurosurgery - Department of Neuroscience and Human Genetics - Meyer Children's Hospital IRCCS, Florence, Italy
University of Florence
flavio.giordano@meyer.it

Matteo Lenge
Neuroscience and Human Genetics Department, Meyer Children's Hospital IRCCS
Florence, Italy
matteo.lenge@meyer.it

***Abstract*— Deep Brain Stimulation (DBS) is a therapeutic strategy for the treatment of dystonia, also in pediatric settings. It acts selectively on deep areas such as the internal Globus Pallidus (GPi). In this study, we report a multimodal analysis carried out on a young patient suffering from generalized dystonia who underwent bilateral DBS implantation at the level of the GPi. The objective was to identify the neurophysiological correlates of dystonia. Through the synchronized recording of deep cerebral (LFP), cortical (EEG), and muscular (EMG) signals, dystonic events were identified and analyzed in different stimulation configurations (including ring mode and directional settings using contacts either proximal to or distal from GPi) and at various levels of stimulation intensity. Spectral analysis was performed on the signals to identify frequency bands associated with dystonic events and to investigate the effects of stimulation. The findings suggest that a personalized approach to DBS may improve the therapeutic management of pediatric dystonia.**

Keywords—Deep Brain Stimulation, Local Field Potential, generalized dystonia, pediatric, EEG, EMG

I. Introduction

Deep Brain Stimulation (DBS) is a neurosurgical technique used in the treatment of Parkinson's disease and essential tremor, also showing efficacy in modulating brain activity in dystonic pediatric patients [1]. Dystonia is a hyperkinetic movement disorder, characterized by sustained and prolonged co-contractions of agonist and antagonist muscles; causing uncontrollable and unwanted torsional movements or abnormal posture assumptions [2][3]. That condition is considered the third most common movement disorder, after Parkinson's and essential tremor [4], and can cause severe motor disability and adversely affect the cognitive and behavioral development of patients. Clinical and experimental evidence points to the basal ganglia as the major site of dysfunction in dystonia [5], with particular involvement of the Globus Pallidus internus (GPi) being a major target for electrode implantation in DBS.

In this study, we developed an analysis pipeline that combines local field potentials (LFP), electroencephalographic (EEG) and electromyographic (EMG) signals and we applied it to a case of a young patient with generalized dystonia undergoing bilateral DBS implantation at the GPi level. Through this approach, we explored the patient's neurophysiological profile, contributing to the understanding of the mechanisms underlying pediatric dystonia and offering insights into possible individualized optimization of stimulation through the integration of surface and deep signals.

II. Materials and Methods

The bilateral DBS was performed under general anesthesia using a frame-based (*Leksell, Elekta Instruments®, Sweden*) technique coupled with a robotic system for stereotactic

neurosurgery (*Neuromate®; Renishaw-Mayfield SA, Nyon, Switzerland*).
The recordings were acquired on the same day during the patient's follow-up hospitalization. Deep brain signals were acquired by the implanted bilateral stimulator (Model B35200 PerceptTM PC Neurostimulator with BrainSenseTM Technology), equipped with two electrodes, one for each brain hemisphere (Fig.1).
Each electrode consists of four segments, two of them with three contacts, for a total of eight contacts per electrode, allowing the configuration of customized and targeted stimulations. In particular, the Ring configuration uses all three contacts of a segment to stimulate uniformly, while directional configurations combine the contacts of different left and right electrode segments to focus the stimulation on a precise area. For the discussion, we will refer to *Directional Configuration close to GPi* as the one involving activation of contacts 0-2 and *Directional Configuration far from GPi* as the one engaging more distant contacts (1-3) on the same electrode lead, where the primary distinction is the set of active contacts used, as illustrated in Fig. 1.

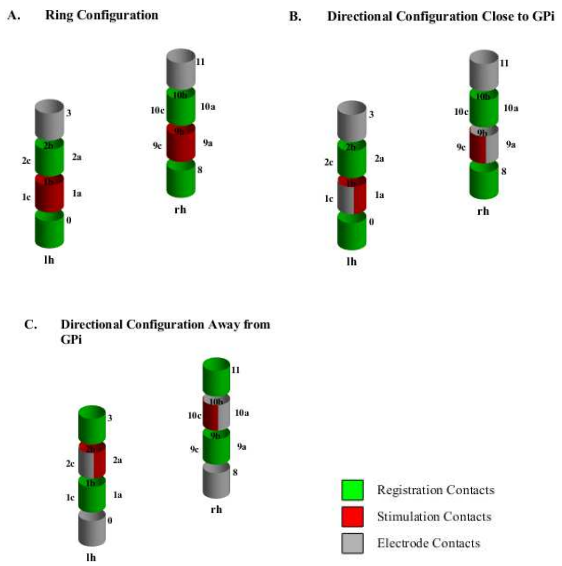

Figure 1. Three-dimensional schematic representation of bilateral electrodes implanted in the right (rh segments 0,1,2,3) and left hemisphere (lh segments 8,9,10,11), respectively. Each electrode consists of four segments, two of which are directional with three contacts, labeled with suffix a,b,c. The proportions and distances between contacts depicted are illustrative and do not reflect the actual dimensions of the device. A) Ring configuration: Recording occurs between segment 0 and 2 on the left and 8 and 10 on the right. Current is delivered from all contacts in segment 1 (1a,1b,1c) and 9 (9a,9b,9c). B) Directional Configuration Close to GPi: Recording occurs between segment 0 and 2 on the left and 8 and 10 on the right. Current is delivered from contacts 1a, 1b and 9c. C) Directional configuration far to the GPi: Recording occurs between segment 1 and 3 on the left and 9 and 11 on the right. Current is delivered from contacts 2a, 2b and 10c.

Surface signals were recorded with a 21-channel EEG system (international standard 10-20, Micromed SRL-Brain Quick BQ 3200) and a surface electromyography system with electrodes placed on flexors and extensors of the upper limbs. The recording session comprises a total of seven acquisitions (LFP, EEG, EMG), each characterized by a different stimulation configuration in terms of active electrode contacts and current intensity. Such variables were chosen by clinicians who considered the positioning of the system and the patient's medical history.

A. LFP

Deep brain signals (local-field potentials, LFP) were exported from the Percept system in JSON format. Each file, containing multiple recordings, is divided into fields including BrainSenseTimeDomain, which reports the raw data of the LFP signal for right hemisphere (rh) and left hemisphere (lh) acquired at 250 Hz, and BrainSenseLfp, which includes the delivered stimulation information recorded at 2 Hz. The BrainSenseLfp section was used to identify the beginning and end of each recording by analyzing timestamps associated with changes in stimulation parameters (Fig. 2A).
Before the synchronization with the surface signals, an integrity check of the LFP packets, acquired by the device in time blocks, was performed. The intervals between consecutive timestamps were analyzed: if the interval exceeded the expected 250 ms, the loss of one or more blocks was supposed. In these cases, to maintain temporal consistency and ensure proper synchronization, dummy packets containing NaN values for both hemispheres were inserted. To ensure synchronization between surface and deep signals, repeated sequences of 2.4 mA stimulation followed by off periods were performed at the beginning of each recording (Fig. 2C, 2E). The sequences were identified superficially by the visibility of the same spike on an additional channel placed on the stimulator case (Fig. 2B, 2D, 2F).
Once synchronization was completed, the dummy elements were removed, along with the corresponding time segments in the other signals. In addition, the initial and final seconds of the stimulation phases were also excluded to prevent stimulation transitions from altering and compromising subsequent analysis.

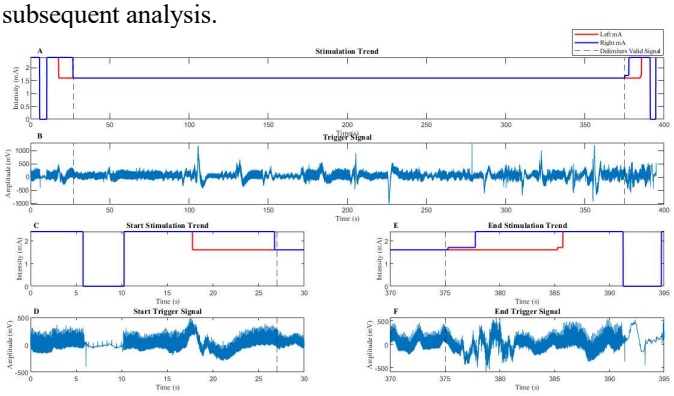

Figure 2: LFP synchronization with surface signals.
Representation of the time course of stimulation intensity and trigger signal, with evidence of state transitions used for synchronization.
(A) Trend of stimulation intensity in milliamps (mA) for the left (red) and right (blue) electrode during the entire recording. Vertical black dashed lines delimit the range of interest defined as valid signal.
(B) Trigger signal synchronized with changes in stimulation parameters.
(C,D) Zoom of the initial phase: in C the ON 2.4 mA, OFF, ON 2.4 mA stimulation current trend; D shows the spikes seen at the stimulation transitions.
(E,F) Zoom of the final phase: in E the trend of stimulation current ON 2.4 mA, OFF, ON 2.4 mA; D shows the spikes seen at the stimulation transitions.

The signals were segmented into consecutive 5-second windows, within which relative power was calculated for each of the five frequency bands [6]: Delta (0.5–4 Hz), Theta (4–8

Hz), Alpha (8–13 Hz), Beta (13–35 Hz), Gamma (35–120 Hz).

B. Surface Signals

Electroencephalographic (EEG) and electromyographic (EMG) signals were acquired with a sampling frequency of 2048 Hz and saved in EDF (European Data Format) for post-processing. To achieve compatibility with LFP signals, the data were resampled at 250 Hz, applying a fourth-order Butterworth-type low-pass filter with a cutoff frequency of 125 Hz. A notch filter was also applied to cancel network interferences. For EEG analysis, 21 channels were selected and referenced against Cz. A FIR filter was applied in the 0.5-45 Hz band. The signals were segmented into consecutive 5-second windows, within which relative power was calculated for each of the five characteristic frequency bands. From the full set of EEG channels, we selected the central derivations, grouped by hemisphere (T3–C3 for the left and T4–C4 for the right), corresponding to the primary motor cortex.

A quantitative EMG approach was adopted for the detection of dystonic events. First, a low-pass filter was applied at 10 Hz [7], the continuous (DC) component was removed and the signal was rectified across the entire recording. For each channel individually, a 4-second segment with the lowest mean power across the entire recording was automatically selected and used as baseline. The signal was then divided into consecutive, non-overlapping 1-second windows. An epoch was considered above threshold if its mean logarithmic power exceeded the baseline by at least one standard deviation, and the power derivative, used to identify sharp changes linked to voluntary movements, remained below the 95th percentile. This allowed the exclusion of transient motor artifacts, focusing only on relevant increases in activity. To increase specificity, only sequences comprising at least four consecutive above-threshold epochs were retained. Segments meeting this criterion were considered candidate activations. Finally, an epoch was defined as “dystonic” if activation was simultaneously present in the flexors and extensors of the same side (Fig. 3). Two expert clinical neurophysiologists reviewed all automatically detected dystonic episodes to verify their validity. Comparing the correctly labeled portions of the signal, the performance of the model was calculated, which achieved an F1 score of 83.3% and a total recall of 90.1%. After correcting the events, those periods in which the mean logarithmic power was comparable to baseline values were labeled as non-dystonic. This conservative approach reduced the risk of including brain signals associated with voluntary movements, thus improving the overall reliability of subsequent analyses.

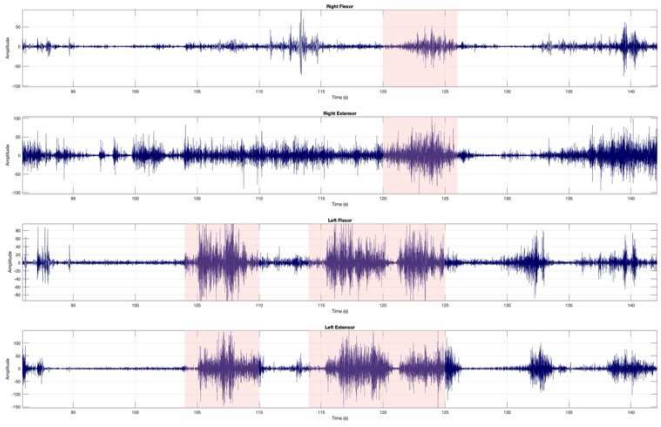

Figure 3. Example of a dystonic event detection for the fourth recording session. In blue the electromyographic signal, pink area identifies the dystonic events identified as flexor and extensor co-contraction on the same side.

C. Spectral Analysis

Analyses were conducted by comparing both superficial and deep brain signals, with electromyographic signals, taking into consideration the principle of contralaterality. However, given the patient's history of generalized dystonia, results will be combined in the conclusions. We began the analysis by calculating Relative Power in LFP and EEG signals, as a measure of spectral activity in the main frequency bands. The first, named Intra-Recording Analysis, compared power changes in EEG and LFP signals during dystonic events versus interictal periods, within the same recording session; the second, called Inter-Recording Analysis, examined power differences during dystonic events under different stimulation conditions.

This analysis was evaluated for three cases:

a. ON-OFF Comparison: Recordings (Ring, Directional Close to and Away from GPi) were grouped together in this first stage of general comparison. For an initial analysis, we limit to distinguishing the presence or absence (OFF protocol) of stimulation, where recordings classified as ON had in common the use of a stimulation current of 1.6 mA regardless of electrode configuration.
b. Directional Close to GPi: Pairwise comparison between stimulator off, low-intensity stimulation (1.6 mA) and high-intensity stimulation (3.2 mA).
c. Directional Away from GPi: Pairwise comparison between stimulator off, low-intensity stimulation (1.6 mA) and high-intensity stimulation (2.4 mA).

D. Statistical Analysis

The statistical analysis, common to the three sections, initially involved checking the normal distribution of the data; in its absence, the nonparametric Mann-Whitney test was applied; the p-values obtained were subsequently corrected using Bonferroni's method. All the analysis have been performed using MATLAB R2024b (Statistics and Machine Learning Toolbox Version 24.2, Signal Processing Toolbox Version 24.2, MathWorks Inc., Natick, MA).

III. Results and Discussion

A. ON-OFF Comparison

The first spectral analysis, performed not considering the presence of dystonic events, showed in LFP in lh a statistically significant increase in delta (lh: $z = -3.72$, $p = 0.001$) and a reduction in beta (lh: $z = 3.59$, $p = 0.003$) and gamma (lh: $z = 11.01$, $p < 0.001$) bands during the stimulation, in the LFPs in the right hemisphere an increase in theta (rh: $z = -3.60$ $p = 0.014$) and alpha (rh: $z = -8.39$ $p = 0.003$) and a reduction in delta (rh: $z = -8.39$, $p < 0.001$) and gamma (rh: $z = 9.78$, $p < 0.001$). We observed a reduction in slow-frequency bands (i.e., delta and theta) in EEG during stimulation (lh: $z = 23.06$, $p < 0.001$; rh: $z = 25.61$, $p < 0.001$; lh: $z = 7.39$ $p < 0.001$; rh: $z = 16.15$, $p < 0.001$, respectively) with an increase in high-frequency bands (i.e., alpha, beta and gamma).

Within the OFF protocol, during the dystonic event, LFPs showed a reduction in slow-frequency bands (i.e., delta (lh: $z = -7.22$, $p < 0.001$) and theta (lh: $z = -6.01$, $p < 0.001$)) and an increase in high-frequency bands, beta (lh: $z = 7.46$, $p < 0.001$) and gamma (lh: $z = 11.33$, $p < 0.001$; rh: $z = 3.82$, $p = 0.001$); We observed no statistical differences in the EEG signal during the dystonic event.

Within the ON protocol for LFP signals we observed a reduction in alpha (lh: $z = -2.81$, $p = 0.04$) and beta (lh: $z = -3.17$, $p = 0.01$) bands, during the dystonic event. Accordingly, the corresponding EEG signal shows an increase in delta (lh: $z = 8.88$, $p < 0.001$) and a decrease in alpha (lh: $z = -10.20$, $p < 0.001$), beta (lh: $z = -9.47$, $p < 0.001$) and gamma (lh: $z = -7.20$, $p < 0.001$) bands.

In Inter-Recording Analysis, comparing relative power during dystonic events, for cortical brain signals, we observed a significant reduction in delta (lh: $z = 7.81$, $p < 0.001$; rh: $z = 9.53$, $p < 0.001$), theta (lh: $z = 3.37$, $p = 0.007$) and a statistically significant increase in all other bands: alpha (lh: $z = -6.77$, $p < 0.001$; rh: $z = -8.22$, $p < 0.001$), beta (lh: $z = -9.44$, $p < 0.001$; rh: $z = -10.65$, $p < 0.001$) and gamma (lh: $z = -10.28$, $p < 0.001$, rh: $z = -11.06$, $p < 0.001$) during the ON protocol compared to the OFF condition. A similar comparison for deep brain signals revealed a different pattern: we observed an increase in slow-frequency bands and a reduction in high-frequency bands: delta (lh: $z = -7.22$, $p < 0.001$), theta (lh: $z = -6.01$, $p<0.001$), beta (lh: $z = 7.46$, $p < 0.001$), gamma (lh: $z=11.33$, $p < 0.001$; rh: $z = 3.58$, $p = 0.003$).

The overall analysis showed an association of the delta band with the dystonic event in the superficial cortical signals and the gamma band in the deep LFP signals, both characterized by enhanced power. Stimulation resulted in a reduction of the respective bands, suggesting the efficacy of the protocol. Specific analysis was then carried out to identify the most suitable configuration for the patient.

B. Directional Close to GPi

This section presents the results of the analysis of the Directional Configuration near the GPi. As shown in Table I, during the dystonic event with stimulation off (0 mA), a statistically significant bilateral increase in the gamma band was observed in deep signals. A similar pattern was seen with the highest current value (3.2 mA). In EEG a significant reduction in the beta band is observed. For both stimulation intensities, the surface signals exhibited a decrease in all high-frequency bands and an increase in the slow-frequency bands.

Spectral analysis, in Table II, showed that with low-intensity stimulation (1.6 mA), compared with stimulation off, there was a significant reduction in the delta band in superficial signals, with a concomitant increase in alpha, beta and gamma in both hemispheres. In contrast, at the deep level, there was a significant rise in the delta and a decrease in the beta band.

Increasing the current to 3.2 mA, compared with off, in the deep signals, there was a significant increase in gamma and beta, associated with a reduction in the delta and theta bands, suggesting lower stimulation efficacy. The superficial signals exhibit a similar pattern to that observed at the lower current level.

The comparison of the two stimulation intensities revealed that as the current increases, in rh the EEG signals showed a significant increase in the delta, accompanied by reductions in alpha, beta, and gamma bands. In contrast, in the deep signals, there was a bilateral rise in gamma, a rise in beta in the right hemisphere and a decrease in the slow band theta in the left hemisphere.

C. Directional Away From GPi

In the configuration away from the GPi (Table III), with the stimulator off, during the dystonic event there is a statistically significant reduction in the theta and alpha bands in the deep signals, and an increase in the gamma, consistent with findings obtained in the proximal configuration with the stimulator off.

When the stimulation was switched on at 1.6mA, inside the dystonic events, we observed a bilateral significant increase in gamma band of deep signals, and a reduction in the alpha, beta and gamma bands is shown in the surface signals, along with an increase in the delta band.

Comparison between stimulation off and the two current intensities (Table IV.) showed, a reduction in delta and an increase in alpha, beta and gamma during the dystonic event in rh the superficial signals, and a bilateral reduction in gamma band, a rise in delta and theta in lh, in the deep signals. Furthermore, the increase in current compared with the stimulator-off condition induced in the deep signals a rise in delta and theta, and an reduction in beta; on the other hand, we observed a reduction in delta and a increase in all other bands in the superficial signals.

Finally, comparing the two stimulation intensities, during dystonic events, the EEG signals reveals the same pattern previously observed in the comparison between 0 and 1.6 mA, only in lh; The LFP signals showed an increase in

theta and delta, and a reduction in beta and gamma bands are detected.

IV. Conclusion

The simultaneous increase in delta-band activity in EEG signals and gamma-band activity in LFP signals aligns with the underlying neurophysiological mechanisms: during dystonic events, there is an increase of GPi firing rate that coincides with lower cortical firing frequency. In the configuration close to the GPi, the reduction in power observed in the frequency bands was associated with the dystonic event—both in cortical and deep signals—when stimulating at 1.6 mA. However, this improvement was not persistent at higher intensities: although stimulation at 3.2 mA might initially seem more effective than at 0 mA, a direct comparison between 1.6 mA and 3.2 mA revealed an increase in delta band power, previously associated with the dystonic event. In contrast, when using the configuration further from the GPi, a progressive improvement is observed even as current intensity increases, which is likely acceptable due to the greater distance from the pathological site.

Although this analysis was conducted on a single patient, constraining the generalizability of the findings, a general improvement following stimulation was observed, as evidenced by spectral analysis and reflected in a reduction in the number of dystonic events. Understanding these mechanisms is essential for guiding personalized treatment strategies, allowing stimulation protocols to be tailored to the specific neurophysiological response of each patient.

Acknowledgment

This research was supported by the National Plan for Complementary Investments to the PNRR Hub Life Science-Digital Health (PNC-E3-2022-23683267, DHEAL COM).

This publication reflects only the authors' view and the Italian Ministry of Health is not responsible for anyuse that may be made of the information it contains.

References

[1] Hale AT, Monsour MA, Rolston JD, Naftel RP, Englot DJ. Deep brain stimulation in pediatric dystonia: a systematic review. Neurosurg Rev. 2020 Jun;43(3):873-880. doi: 10.1007/s10143-018-1047-9. Epub 2018 Nov 5. PMID: 30397842; PMCID: PMC6500764

[2] Fahn S. Concept and classification of dystonia. Adv Neurol. 1988;50:1-8. PMID: 3041755.

[3] Vogt, L. M., Yang, K., Tse, G., Quiroz, V., Zaman, Z., Wang, L., Srouji, R., Tam, A., Estrella, E., Manzi, S., Fasano, A., Northam, W. T., Stone, S., Moharir, M., Gonorazky, H., McAlvin, B., Kleinman, M., LaRovere, K. L., Gorodetsky, C., & Ebrahimi-Fakhari, D. (2024). Recommendations for the Management of Initial and Refractory Pediatric Status Dystonicus. In *Movement Disorders*. John Wiley and Sons Inc.

[4] Fan, H., Zheng, Z., Yin, Z., Zhang, J., & Lu, G. (2021). Deep Brain Stimulation Treating Dystonia: A Systematic Review of Targets, Body Distributions and Etiology Classifications. In *Frontiers in Human Neuroscience* (Vol. 15). Frontiers Media S.A.

[5] Primary dystonia and dystonia-plus syndromes: clinical characteristics, diagnosis, and pathogenesis. Phukan, Julie et al. The Lancet Neurology, Volume 10, Issue 12, 1074 - 1085

[6] Local field potentials: Therapeutic implications for DBS in dystonia including adaptive DBS for dystonia, Ledingham, David et al., Deep Brain Stimulation, Volume 5, 4 - 19

[7] Merletti, Roberto, and Dario Farina, eds. *Surface electromyography: physiology, engineering, and applications*. John Wiley & Sons, 2016.

[8] Dressler, D. "Electromyographic evaluation of cervical dystonia for planning of botulinum toxin therapy." *European Journal of Neurology* 7.6 (2000): 713-718.

TABLE I.

Intra-Registration Analysis Close To GPi		**Power Bands**									
		Delta (z, p)		**Theta (z, p)**		**Alpha (z, p)**		**Beta (z, p)**		**Gamma (z, p)**	
		LFP	**EEG**	**LFP**	**EEG**	**LFP**	**EEG**	**LFP**	**EEG**	**LFP**	**EEG**
OFF	lh	-1.37 1.000	-0.96 1.000	**-3.29** **0.009**	1.48 1.000	-0.41 1.000	0.42 1.000	1.61 1.000	0.50 1.000	**6.45** **<0.001**	0.44 1.000
	rh	-0.48 1.000	1.78 0.753	-1.36 1.000	1.17 1.000	-0.47 1.000	-1.86 0.619	0.12 1.000	**-2.91** **0.037**	**3.83** **<0.001**	-2.50 0.123
1.6 mA	lh	1.32 1.000	**7.54** **<0.001**	1.39 1.000	**4.93** **<0.001**	-1.05 1.000	**-6.87** **<0.001**	**-3.09** **0.019**	**-8.88** **<0.001**	0.97 1.000	**-8.51** **<0.001**
	rh	1.74 0.871	1.81 0.759	0.38 1.000	**3.68** **0.003**	-1.03 1.000	-0.23 1.000	-2.39 0.180	-2.58 0.108	-0.45 1.000	-2.65 0.09
3.2 mA	lh	1.01 1.000	-0.46 1.000	-2.10 0.362	1.43 1.000	-1.77 0.783	-0.59 1.000	-0.58 1.000	-0.96 1.000	0.95 1.000	-1.04 1.000
	rh	-2.73 0.063	**4.44** **<0.001**	-2.36 0.184	**5.87** **<0.001**	-1.15 1.000	-2.69 0.070	2.40 0.163	**-5.49** **<0.001**	**5.31** **<0.001**	**-5.53** **<0.001**

TABLE II.

Inter-Registration Analysis Close to GPi		**Power Bands**									
		Delta (z, p)		**Theta (z, p)**		**Alpha (z, p)**		**Beta (z, p)**		**Gamma (z, p)**	
		LFP	**EEG**	**LFP**	**EEG**	**LFP**	**EEG**	**LFP**	**EEG**	**LFP**	**EEG**
0-1.6 mA	lh	**-2.99 0.028**	**5.67 <0.001**	-2.09 0.367	-2.58 0.098	-0.11 1.000	**-5.78 <0.001**	**4.12 <0.001**	**-5.73 <0.001**	**7.21 <0.001**	**-6.17 <0.001**
	rh	-0.94 1.000	**3.92 0.001**	0.38 1.000	**-3.60 0.003**	-0.52 1.000	**-3.95 0.001**	0.87 1.000	**-3.82 0.001**	2.56 0.104	**-3.92 0.001**
0-3.2 mA	lh	-1.46 1.000	2.06 0.391	1.93 0.531	-0.28 1.000	1.47 1.000	-2.12 0.341	1.18 1.000	**-3.17 0.015**	1.78 0.749	**-5.65 <0.001**
	rh	**4.18 <0.001**	**7.60 <0.001**	**4.88 <0.001**	-0.13 1.000	-0.98 1.000	**-5.57 <0.001**	**-4.63 <0.001**	**-7.94 <0.001**	**-3.36 0.008**	**-9.71 <0.001**
1.6-3.2 mA	lh	1.49 1.000	**-5.32 <0.001**	**4.44 <0.001**	2.86 0.042	1.74 0.820	**5.42 <0.001**	**-3.82 0.048**	**4.63 <0.001**	**-4.46 <0.001**	**3-22 0.013**
	rh	1.88 0.609	-1.79 0.733	1.31 1.000	2.67 0.075	0.35 1.000	2.56 0.105	-2.19 0.290	1.51 1.000	**-3.02 0.025**	1.26 1.000

TABLE III.

Intra-Registration Analysis Away from GPi		**Power Bands**									
		Delta (z, p)		**Theta (z, p)**		**Alpha (z, p)**		**Beta (z, p)**		**Gamma (z, p)**	
		LFP	**EEG**	**LFP**	**EEG**	**LFP**	**EEG**	**LFP**	**EEG**	**LFP**	**EEG**
OFF	lh	-2.50 0.125	-1.61 1.000	**-4.38 <0.001**	2.20 0.215	**-4.39 <0.001**	2.04 0.421	1.45 1.000	0.45 1.000	**6.79 <0.001**	0.96 1.000
	rh	0.99 1.000	-0.23 1.000	**-2.98 0.028**	0.32 1.000	**-4.37 <0.001**	-0.06 1.000	0.08 1.000	-0.30 1.000	**3.29 0.009**	0.81 1.000
1.6 mA	lh	-0.29 1.000	**5.21 <0.001**	-1.45 1.000	1.17 1.000	-2.12 0.340	**-4.87 <0.001**	0.65 1.000	**-6.42 <0.001**	**3.33 0.008**	**-6.93 <0.001**
	rh	-0.67 1.000	0.07 1.000	-2.46 0.140	1.89 0.591	-2.29 0.220	0.41 1.000	1.39 1.000	-0.99 1.000	**4.07 <0.001**	-0.47 1.000
3.2 mA	lh	1.16 1.000	-1.79 0.775	-0.63 1.000	2.16 0.328	-2.21 0.287	1.95 0.544	-0.79 1.000	1.05 1.000	1.79 0.774	0.32 1.000
	rh	0.92 1.000	-1.78 0.764	0.57 1.000	2.45 0.142	-2.26 0.240	2.23 0.257	-1.14 1.000	0.52 1.000	1.64 1.000	-1.36 1.000

TABLE IV.

Inter-Registration Analysis Away from GPi		**Power Bands**									
		Delta (z, p)		**Theta (z, p)**		**Alpha (z, p)**		**Beta (z, p)**		**Gamma (z, p)**	
		LFP	**EEG**	**LFP**	**EEG**	**LFP**	**EEG**	**LFP**	**EEG**	**LFP**	**EEG**
0-1.6 mA	lh	**-3.24 0.012**	0.64 1.000	**-3.45 0.005**	-0.33 1.000	-1.86 0.628	-0.62 1.000	1.53 1.000	-2.16 0.308	**5.51 <0.001**	-2.04 0.417
	rh	-0.33 1.000	**4.63 <0.001**	0.62 1.000	-1.17 1.000	-0.17 1.000	**-4.51 <0.001**	-1-09 1.000	**-5.58 <0.001**	0.88 1.000	**-5.55 <0.001**
0-3.2 mA	lh	**-4.98 <0.001**	**4.58 <0.001**	**-6.25 <0.001**	**-3.88 0.002**	-2.07 0.386	**-4.74 <0.001**	**4.75 <0.001**	**-4.94 <0.001**	**7.36 <0.001**	**-5.24 <0.001**
	rh	**-4.77 <0.001**	**4.77 <0.001**	**-5.71 <0.001**	**-3.98 0.001**	-1.15 1.000	**-4.44 <0.001**	**5.27 <0.001**	**-4.15 0.001**	**7.15 <0.001**	**-3.35 0.008**
1.6-3.2 mA	lh	2.04 0.420	**3.76 0.002**	**-3.23 0.012**	**-3.31 0.009**	-0.30 1.000	**-3.91 0.009**	**3.18 0.015**	**-3.28 0.010**	**3.15 0.016**	**-3.59 0.003**
	rh	**-3.34 0.008**	-1.77 0.775	**-4.56 <0.001**	-1.57 1.000	0.62 1.000	1.54 1.000	**4.96 <0.001**	**2.97 0.030**	**4.94 <0.001**	**3.75 0.002**